Determination of the fluorescence quantum yield by oceanic phytoplankton in their natural habitat

Stéphane Maritorena, André Morel, and Bernard Gentili

Sun-stimulated chlorophyll *a* fluorescence has been measured *in situ*, within the upward and downward light fields, in oceanic waters with chlorophyll concentrations of 0.04–3 mg m^{-3}. We combined these signals with phytoplankton absorption spectra to derive the fluorescence quantum yield, ϕ (number of photons emitted by fluorescence/number of absorbed photons). ϕ was derived separately from hyperspectral (upward and downward) irradiance measurements (with a LI-COR Instruments spectroradiometer) and from nadir radiance near 683 nm (with a Biospherical Instruments profiler). The contribution of inelastic Raman scattering to the signal in the red band was assessed and subtracted. Raman-corrected ϕ values derived from the two instruments compared well. Vertical ϕ profiles were strongly structured, with maximal (5–6%) values at depth, whereas ϕ was $\cong$1% in near-surface waters (measurements made approximately at solar noon). These near-surface values are needed for interpretation of remotely sensed fluorescence signals. This optical study shows that the fluorescence yield of algae in their natural environment can be accurately derived in a nonintrusive way with available instrumentation and adequate protocols.

OCIS codes: 010.4450, 260.2510.

1. Introduction

Although it was not identified as such, solar-stimulated fluorescence of chlorophyll *a* was likely observed for the first time by Tyler and Smith in 1967,[1] in the San Vincente reservoir near San Diego, Calif. The upwelling irradiance spectra, measured at depths from 1 to 6 m within this body of water, distinctly showed a relative, Gaussian shaped, maximum in the red part of the spectrum.[1] Later, this feature centered about 685 nm was repeatedly detected in nadir radiance signal or in subsurface reflectance and was independently interpreted as fluorescence emission by chlorophyll-bearing cells.[2,3] This attribution was confirmed by Gordon,[4] who showed that the enhancement of reflectance near 685 nm can be fully accounted for by Sun-induced *in vivo* fluorescence of living algal cells; he also concluded that, even if the yield of this process remains low, the emission is significant and detectable (see also Kattawar and Vastano[5]). The yield is simply defined as the ratio of the amount of energy (or number of photons) emitted to the energy (or photons) absorbed. Thereafter, systematic observations of the fluorescence signal in the upward irradiance field were carried out and reported.[6] On the basis of these measurements, estimates of the *in situ* quantum yield of chlorophyll fluorescence were derived in different locations and at various depths in the water column.[7] Kiefer *et al*.[8] built a submersible radiometer specifically designed to measure the "natural fluorescence" (the term that they coined for solar-induced chlorophyll fluorescence) throughout the euphotic zone. Following ideas developed by Falkowski and Kiefer,[9] possible relationships between this fluorescence signal and the size and photosynthetic rate of the algal crop were investigated.[10] Topliss and Platt[11] also examined such potential applications.

Simultaneously, it was acknowledged that quantitative interpretation of *in vivo* fluorescence data is still hampered by insufficient information about the processes that control the fluorescence yield of natural phytoplanktonic populations in their environment.[12] Laboratory studies of fluorescence that use isolated chloroplasts or cell preparations under external illumination are numerous, and the significance

S. Maritorena (stephane@icess.ucsb.edu) is with the Institute for Computational Earth System Science, University of California at Santa Barbara, Santa Barbara, California 93106-3060. A. Morel (morel@obs-vlfr.fr) and B. Gentili are with the Laboratoire de Physique et Chimie Marines, Université Pierre and Marie Curie and Centre National de la Recherche Scientifique, Quai de la Darse, BP 8, 06238 Villefranche-sur-Mer cedex, France.

Received 16 March 2000; revised manuscript received 20 September 2000.

0003-6935/00/366725-13$15.00/0

of the fluorescence process in plant physiology is broadly understood (see, e.g., the review by Krause and Weis[13]). In contrast, *in situ* determinations of the fluorescence yield by intact phytoplanktonic organisms in their habitat remain rather scarce. The variations of this yield under various natural conditions are also poorly documented.

The derivation of the yield requires, besides accurate quantification of the fluorescence signal, that the spectral composition of exciting energy as well as the spectral absorption capability of phytoplankton be known. These requirements could not be fulfilled in the absence of determination of algal absorption or with the nonspectral prototype instrument developed by Kiefer *et al*.[8] They were partly satisfied in the experiments of Kishino *et al*.[7] that included detailed spectral (upward) irradiance measurements and the use of three generic phytoplankton absorption spectra that were assumed to be typical of the three locations investigated.

The present study takes advantage of the simultaneous deployment of two instruments, namely, a spectroradiometer (LI-COR Instruments Model LI-1800 UW) which measures spectral irradiance at discrete depths, and a Biospherical Instruments (Model PNF 300) profiler, which continuously measures the fluorescence signal (and actually derives from the prototype of Kiefer *et al*.[8] mentioned above). It also takes advantage of the combination of these optical measurements with systematic determinations made at various depths in the same locations of the absorption spectra of living phytoplankton. Knowledge of the algal absorption allows separate estimates of the fluorescence quantum yield to be made from the data provided by each instrument. Making this derivation and comparing the two estimates are the first aims of this study. In passing, deriving ϕ from the PNF 300 profiler (combined with actual algal absorption) is not the usual way to use the data provided by this device. On the contrary, the product of ϕ and algal absorption is commonly assumed to be constant, so under this coarse assumption a chlorophyll concentration profile is straightforwardly derived from the fluorescence signal profile.

The red fluorescence peak can be detected not only in the upward irradiance field but also in the downward radiant field, provided that the depth is sufficient and that the spectral information is detailed and accurate (as it is in the case with the LI-1800 UW instrument). As far as we know, concomitant observations of the fluorescence emission in both directions were not explicitly reported before. In the red spectral domain the fluorescence signal is inevitably intermingled with the inelastic Raman scattering. Therefore the respective contributions of these two processes to radiation near 685 nm are to be quantitatively assessed in natural conditions. That assessment is a further aim of the present study; in its absence the estimate of the fluorescence yield is necessarily biased. For example, ignoring the Raman contribution and interpreting the PNF 300 red signal directly in terms of algal fluorescence necessarily lead to an overestimate of this emission and consequently of the yield of this process.

With the data in hand, it is possible to derive ϕ and to calculate its change with depth or location. However, the physiological implications of this change, as a response to environmental factors (such as light and nutrients), and the ecological interpretation of it in terms of algal assemblage are beyond the scope of the present study, which is essentially limited to optical aspects. Our main goal is to demonstrate that the variations in ϕ can be accurately captured with available instrumentation and through nonintrusive methods. Special attention is paid to the ϕ values near the surface compared with those at depth. Indeed, knowledge of subsurface values is required for interpretation of airborne remotely sensed fluorescence data[14] and for deriving the chlorophyll concentration within the upper layer of the ocean from the fluorescence signature detected by spaceborne sensors such as MODIS[15] and MERIS.[16]

2. Instruments and Methods

The PNF 300 profiler (Biospherical Instruments) and the LI-1800 UW spectroradiometer (LI-COR Instruments) were attached to each other and simultaneously immersed. The PNF 300 is a submersible instrument that aims in the nadir direction and measures the upwelling radiance within a spectral domain (665–740 nm, approximately) that encompasses the chlorophyll *a* fluorescence emission band. This radiance, called Lu683, is expressed in units of quanta m^{-2} s^{-1} sr^{-1}. Simultaneously, the scalar irradiance $\mathring{E}_{PAR}$ [quanta m^{-2} s^{-1}] is measured for the whole photosynthetically active radiation domain (PAR; the 400–700-nm band, approximately). Both signals are recorded in a continuous way, and vertical profiles of Lu683 and $\mathring{E}_{PAR}$ are obtained (Fig. 1). Another PAR sensor monitors the solar radiation incident upon the deck and thus allows the slight shift in incident radiation during the experiment to be corrected for.

The LI-1800 UW underwater spectroradiometer measures plane irradiance from 305 to 800 nm with a spectral resolution of 8 nm. Downward and upward spectral irradiance, $E_d(\lambda)$ and $E_u(\lambda)$, respectively, were measured during two successive casts. These casts were performed in rapid succession, one with the flat collector receiving the downward flux and the other after the instrument had been turned upside down. The data, recorded every 5 nm, are expressed in units of W m^{-2} s^{-1} nm^{-1} (or quanta m^{-2} s^{-1} nm^{-1}); they were also corrected for changing irradiance at the surface by use of the same PAR sensor mentioned above. Therefore all the spectra, $E_d(\lambda)$ as well as $E_u(\lambda)$, recorded at various depths were normalized by the same above-water irradiance and are thus directly compatible with the simultaneous PNF 300 data at the same depth. The measurements were generally made in excellent conditions, near solar noon and under perfectly or almost cloudless skies. Normalization of all radiometric data to a

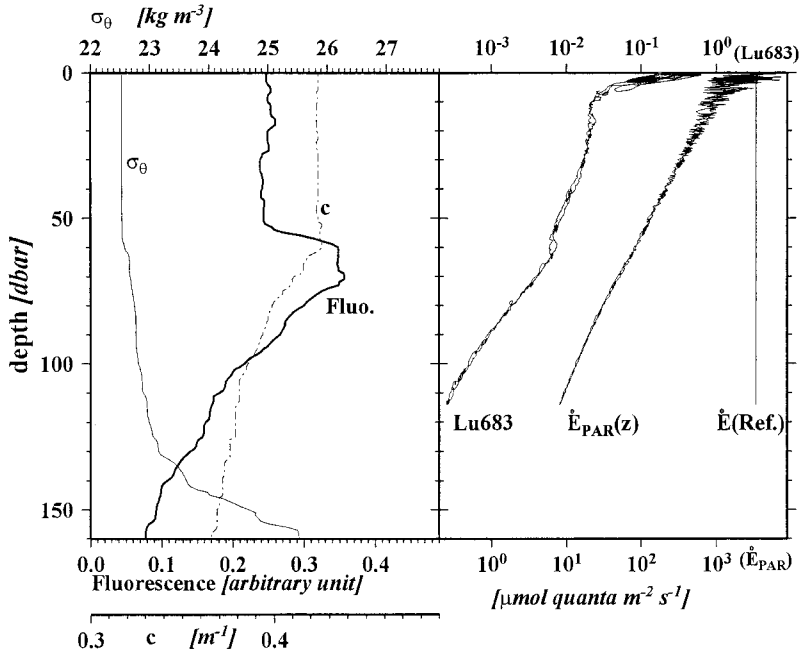

Fig. 1. OLIPAC Station 7, 150 °W–4 °S (12 November 1994). Left, vertical profiles of beam attenuation and fluorescence (SeaTech sensors) and density excess. Right, vertical profiles obtained with the PNF 300 instrument (downcasts and upcasts); note the different scales used for Lu683 and for $\dot{E}_{\mathrm{PAR}}$ (at depth or above surface).

constant above-surface irradiance was thus easy and accurately achieved.

Whereas the PNF 300 sensor can perform measurements in a continuous way and thus provides vertical profiles, the LI-1800 UW instrument must be stopped at discrete depths for determination of spectral irradiance (scanning a spectrum takes ~25 s). The protocol was always to lower the package continuously to a maximum depth (100 m or more) and then to stop it at selected levels during the upcast and operate the hyperspectral instrument. Fluctuations caused by surface waves and lens effects prevented the measurement of $E_d(\lambda)$ within the upper layer. Noise-free spectra were in general successfully recorded only when depth exceeded 20–25 m in clear waters. In contrast, there was no noise in the $E_u(\lambda)$ determinations, even close to the surface. The nominally selected depths (increments of 5 or 10 m) were the same for the E_d and E_u measurements, but in practice these depths were slightly different from those of E_d and E_u (often by less than 1 m), as measured by the pressure gauge. For comparison, the $E_d(\lambda)$ spectrum was (logarithmically) interpolated between the two depths that bracket $E_u(\lambda)$ in such a way that upwelling and downwelling irradiance spectra were at exactly the same depth.

The absorption spectra of total particulate matter, collected onto glass-fiber filters, were determined by a wet-filter technique and corrected for the path-length amplification effect.[17,18] Absorption spectra for nonalgal material were determined by a chemical extraction method[19] or a numerical decomposition technique.[20] We derived the phytoplankton absorption spectra needed for the present study by subtracting the nonalgal absorption from the particulate absorption. The sampling for absorption and pigment determination was normally effected twice, before and after the optical cast; nominally eight depths from 5 to 105 m were sampled. These sampling depths generally did not coincide exactly with those of the irradiance measurements. When needed, a simple linear procedure was applied such that we could infer the absorption spectrum at the level of the optical determination or even produce a quasi-continuous vertical profile of the absorbed radiation (to be associated with the PNF 300 profiles). Pigment determinations were made for the same samples by a high-performance liquid chromatography technique.[21]

The description above is related to the instruments and methods that were employed during a cruise in the tropical central Pacific Ocean (see below). Data from another cruise, in the rich waters of the Peru upwelling area, are also examined in the present study (see below). Methods used during the second cruise were slightly different from those of the first, as here a custom-built spectroradiometer was used for $E_d(\lambda)$ and $E_u(\lambda)$ measurements and there was no sensor equivalent to the PNF 300 instrument. The pigment determinations were made through conventional spectrophotometric or fluorometric methods, whereas the absorption spectra[20] were measured as for the central Pacific, although in a less systematic manner (with respect to depth). For the sake of completion in terms of chlorophyll range and trophic state, data from the near-surface layer of the Peru upwelling cruise are comparatively examined.

3. Locations and Cruises

The OLIPAC (Oligotrophie en Pacifique) cruise, in November 1994, consisted of a south–north transect along the 150 °W meridian from 13 °S to 1 °N, with 11 daily stations, and then of two 5-day stations, at 5° and 16 °S.[21,22] Extreme oligotrophic conditions prevailed in the southernmost locations, with chlorophyll concentration [Chl] always below 0.1 mg m^{-3} in the upper layers, above a deep (100–140-m) chlorophyll maximum (DCM), where the [Chl] slightly exceeded 0.25 mg m^{-3}. The oligotrophic character of these oceanic waters progressively diminished northward; near the equator the situation was drastically different, with an algal biomass uniformly distributed along the vertical, and [Chl] values near 0.3 mg m^{-3}. The PACIPROD (Pacifique Productivity) cruise (first leg in August 1986) started from the Peruvian upwelling area near Cabo Nasca and ended in Guayaquil, Ecuador.[23] In this zone, mesotrophic to eutrophic waters were regularly encountered from offshore to near-shore stations, with [Chl] values ranging from 0.85 to 4.5 mg m^{-3}. Even near the Peruvian coast, where the highest [chlorophyll concentrations] were observed, the waters were case 1 waters.[24]

4. General Background

The flux, F_f [W m^{-3}], emitted by an elementary volume containing a fluorescing substance is related to the flux absorbed by this substance, A_{ex} [W m^{-3}], by means of a yield denoted ϕ, through

$$F_f = \phi A_{ex}. \tag{1}$$

The fluorescence emission is isotropic and takes place within a spectral domain denoted Λ_{em}; the spectral domain that contains the excitation wavelengths is denoted Λ_{ex}. When one is dealing with planktonic algae and chlorophyll *a* fluorescence, the flux absorbed at the depth considered, z, can be expressed as

$$A_{ex} = [\mathrm{Chl}] \int_{\Lambda_{ex}} a^*(\lambda)\mathring{E}(\lambda)\mathrm{d}\lambda, \tag{2}$$

where $\mathring{E}(\lambda)$ is the spectral scalar irradiance at this depth, [Chl] is the local chlorophyll concentration [mg m^{-3}], and $a^*(\lambda)$ is the chlorophyll-specific absorption coefficient of phytoplankton [m^2 mg^{-1}]; the integration is performed over the Λ_{ex} domain.

In Eq. (1), ϕ is a realized yield. It may, and generally does, differ from the true physiological yield. Indeed, partial reabsorption of the emitted light may occur inside the organism before this light can escape[16,25] in such a way that the realized yield is less than the true yield. In what follows, only this realized yield is computed and discussed.

Equation (2) can conveniently be condensed to

$$A_{ex} = [\mathrm{Chl}]\bar{a}^*_{ex}\mathring{E}_{ex}. \tag{2'}$$

If, in Eq. (1), F_f and A_{ex} are both expressed in quantum units [mol quanta m^{-3} s^{-1}], ϕ is the fluorescence quantum yield, namely, the ratio of the number of photons emitted per number of photons absorbed. In this case the spectrally weighted specific absorption coefficient of phytoplankton $\bar{a}^*_{ex}$ [which appears in Eq. (2′)] has to be computed according to

$$\bar{a}^*_{ex} = \int_{\Lambda_{ex}} a^*(\lambda)\mathring{E}(\lambda)\lambda\mathrm{d}\lambda \Big/ \int_{\Lambda_{ex}} \mathring{E}(\lambda)\lambda\mathrm{d}\lambda, \tag{2''}$$

where the denominator represents $\mathring{E}_{ex}$ expressed in quantum units. In what follows, the fluorescence yield is always computed and discussed on a quantum basis.

A. Fluorescence Yield from Nadir Radiance

A thin water layer of thickness dx, located at a distance x below the sensor (located at a depth z), produces by fluorescence an elementary radiance d$L_f(x)$:

$$\mathrm{d}L_f(x) = (1/4\pi)F_f(x)\mathrm{d}x, \tag{3}$$

where the factor $(1/4\pi)$ accounts for the isotropic character of the fluorescence emission.

Now, the excitation flux at x is related to that at the sensor level ($x = 0$) through

$$\mathring{E}_{ex}(x) = \mathring{E}_{ex(x=0)}\exp(-K_{ex}x), \tag{4}$$

where $\mathring{E}_{ex\,(x=0)}$ represents the scalar irradiance for the entire spectral domain Λ_{ex}, and K_{ex} (denoted simply K hereafter) is the attenuation coefficient for this polychromatic scalar irradiance. The elementary radiance d$L_f(x)$ is attenuated when it is traveling upward along distance x to reach the sensor. In the spectral domain that corresponds to the chlorophyll fluorescence emission (near 685 nm), scattering is negligible compared to absorption, and in fact absorption results essentially from the water itself and is rather high.[26] Therefore the diffuse attenuation coefficient that affects d$L_f(x)$ practically reduces to the absorption coefficient[8] and by approximation is simply written as $\exp(-a_{em}x)$, where a_{em} is the mean water absorption coefficient for the spectral domain that corresponds to the chlorophyll fluorescence emission, Λ_{em}. At the level of the sensor (i.e., at $x = 0$), radiance d$L_f(z)$, which originates from the layer at x, is thus expressed as

$$\mathrm{d}L_f(z) = (\phi/4\pi)\mathring{E}_{ex}(z)\bar{a}_{ex}\exp[-(a_{em} + K)x]\mathrm{d}x, \tag{5}$$

where $\bar{a}_{ex} = [\mathrm{Chl}]\bar{a}^*_{ex}$ [see Eq. (2′)]. We then obtain the total fluorescence signal received by the sensor, $L_f(z)$, by integrating Eq. (5) with respect to x, from 0 to (in principle) infinity. In practice, because a_{em} is large, L_f is essentially created by the nearest layers (see below), so ϕ can be safely assumed to be constant and left outside the integral. In the same way, $\bar{a}_{ex}$, a_{em}, and K can be considered constant over the depth interval involved in the integration. Therefore, un-

der these reasonable assumptions, integrating Eq. (5) simply leads to

$$L_f(z) = (\phi/4\pi)\mathring{E}_{ex}(z)\bar{a}_{ex}(a_{em} + K)^{-1}. \quad (6)$$

Equation (6) is equivalent to Eq. (17) of Kattawar and Vastano.[5]

B. Fluorescence Yield from Upward and Downward Plane Irradiances

The contributions of fluorescence to the irradiances $E_d(\lambda)$ and $E_u(\lambda)$, once they are integrated over the Λ_{em} spectral domain, are denoted $E_{f\downarrow}$ and $E_{f\uparrow}$, respectively. As the fluorescence emission is isotropic, the flux that is exiting a horizontal layer is πL, and Eq. (6) thus becomes

$$E_{f\uparrow}(z) = (\phi/4)\mathring{E}_{ex}(z)\bar{a}_{ex}(\kappa + K)^{-1}, \quad (7)$$

where κ replaces a_{em} and represents an attenuation coefficient for the irradiance generated by fluorescence and propagating upward. This coefficient, similar to the κ defined by Kirk[27] for elastically backscattered radiation, is equal to that considered for radiation reflected by a Lambertian reflecting bottom.[28] An analytical approach or Monte Carlo simulations show that its value is 1.5 a_{em}, a value that is also used by Marshall and Smith[29] for the Raman emission.

For the fluorescence contribution to downward irradiance, the sign in Eq. (4) is reversed as the layers above the instrument are increasingly lit when distance (x) from the sensor increases (conversely to what happens for $E_{f\uparrow}$), so $\exp(-K_{ex}x)$ becomes $\exp(+K_{ex}x)$, whereas κ remains unchanged. Therefore, when one is dealing with the downward flux and the $E_{f\downarrow}$ signal, Eq. (7) becomes

$$E_{f\downarrow}(z) = (\phi/4)\mathring{E}_{ex}(z)\bar{a}_{ex}(\kappa - K)^{-1}. \quad (8)$$

In writing Eq. (8) it must be also assumed that the water layers above the instrument (and thus the upper limit for integration) are not limited by the presence of the air–water interface; consequently this expression is valid far enough from the surface (see below). The asymmetry factor between the two signals is described by the ratio

$$E_{f\downarrow}(z)/E_{f\uparrow}(z) = (\kappa + K)/(\kappa - K). \quad (9)$$

Note that one can also directly obtain the factor 1/4 in Eqs. (7) and (8) by considering that the average cosine for the isotropic emission is 1/2 and that only half of the yield is involved when the upper and lower half-spaces are separately considered.

If the two signals are added,

$$[E_{f\downarrow}(z) + E_{f\uparrow}(z)] = (\phi/2)\mathring{E}_{ex}(z)\bar{a}_{ex}\kappa/(\kappa^2 - K^2). \quad (10)$$

C. Numerical Aspects

The chlorophyll fluorescence emission is approximately Gaussian in shape, centered at 683–685 nm, with a half-height width of ~25 nm. In this spectral domain, absorption that is due to water molecules is predominant in oceanic waters. We can obtain the mean absorption coefficient a_{em} by considering the pure-water absorption spectrum[26] convoluted with the Gaussian curve, which yields $a_{em} = 0.495\ m^{-1}$. In case 1 waters, the increment that is due to the presence of biological materials is less than $0.02\ m^{-1}$ when the [Chl] is 1 mg m^{-3}. The mean a_{em} value adopted is simply $0.51\ m^{-1}$ and is $0.76\ m^{-1}$ for κ.

The attenuation coefficient K for scalar irradiance is close to the coefficient for downward irradiance over the same Λ_{ex} spectral range; it is thus derived from the $E_d(\lambda)$ measurements. For the OLIPAC cruise, K lies at 0.035–0.055 m^{-1}, depending on depth and location. The sum and difference $(\kappa + K)$ and $(\kappa - K)$ take, on average, the values 0.80 and 0.72 m^{-1}, respectively. With such K and κ values it is easy to see [by integrating Eq. (5) up to 90% of its final value, which is reached when x tends toward infinity] that 90% of the fluoresced photons in the upward flux originate from a 2.9-m-thick layer below the sensor [Eq. (6) or (7)]. Within the downward flux, 90% of the fluorescence comes from a 3.2-m-thick layer above the sensor; therefore Eq. (8) becomes valid beyond this depth, and, practically (because of limitations owing to fluctuations), it will never be used at depths less than 30 m. For the PACIPROD stations the actual K values are higher and range from 0.11 to 0.21 m^{-1}; they are used on a case-by-case basis, whereas κ is kept unchanged.

The limit of the excitation spectral range, Λ_{ex}, toward the short-wavelength region is not well known; it is set at 370 nm. In the red part of the spectrum, the excitation and emission domains partly overlap, and reabsorption may occur. The upper limit for Λ_{ex} is arbitrarily set at 655 nm and emission domain Λ_{em} is bounded by wavelengths of 655 and 710 nm.

When it is needed, scalar irradiance is derived from downward plane irradiance. One makes this transformation simply by applying a constant factor equal to 1.30 to the downward irradiance. In fact this geometric factor, which depends on wavelength, depth, and illumination conditions above the surface, can be computed from the radiative transport equation.[30] The value given above is an approximation for the conditions encountered during the experiments analyzed below and for the whole (Λ_{ex}) spectral domain. Considering other experimental sources of uncertainties, this approximation seems amply sufficient.

D. Description of the Data

The various kinds of optical measurement (upward and downward irradiances, nadir radiance data, spectral and nonspectral determinations) from the OLIPAC cruise were used for the present study. For the PACIPROD cruise, among the E_u spectra, only those determined just beneath the surface were considered. Including these near-surface data allows the chlorophyll range to be widely extended toward high values, in particular for remote-sensing applications. Typical examples of the fluorescence data analyzed in the present study are displayed in Figs. 1 and 2. Figure 1 shows the vertical profiles of E_{PAR}

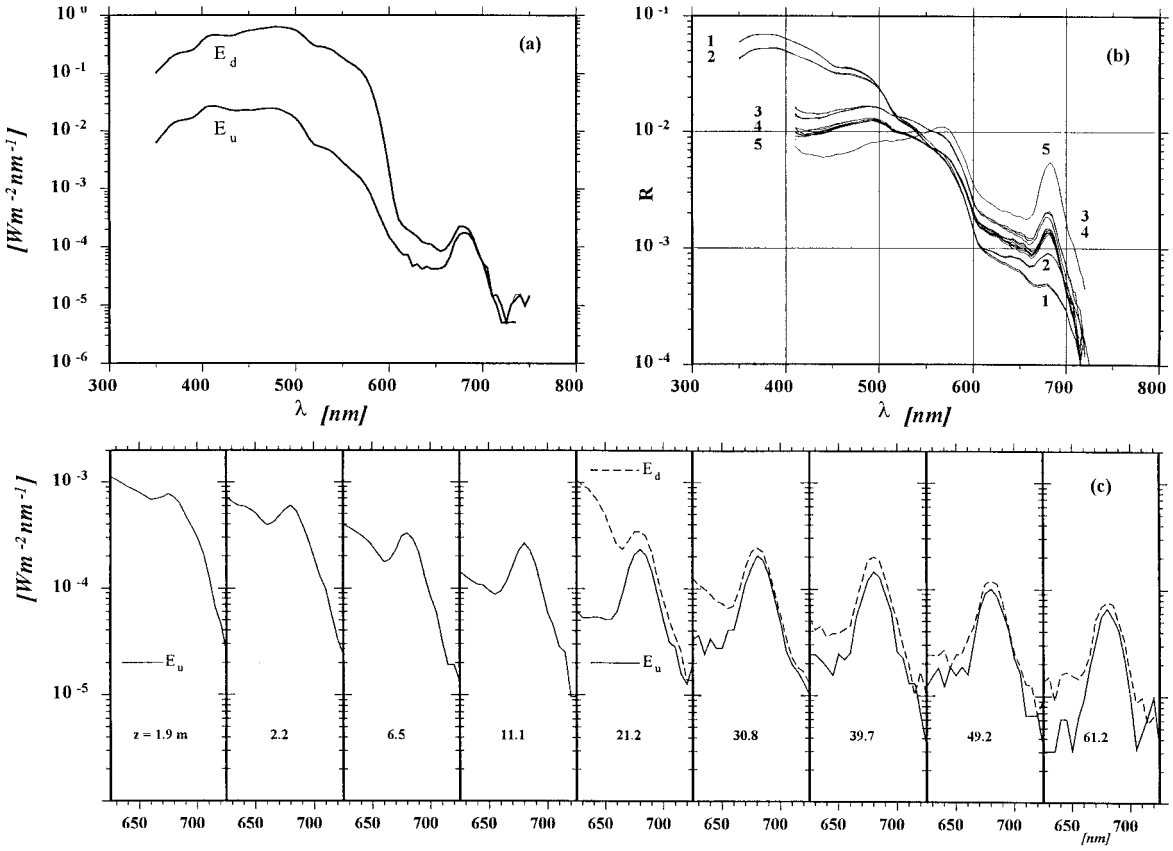

Fig. 2. (a) Examples of upward and downward irradiance spectra (logarithmic scale, Station 3, 150 °W–10 °S, 8 November 1994) determined at 31.6 m; the chlorophyll concentration at this depth is 0.09 mg m^{-3}. (b) Reflectance spectra for two stations (OLIPAC cruise), denoted 1 and 2, with [Chl] = 0.09 and [Chl] = 0.17 mg m^{-3}, respectively, and three stations (PACIPROD cruise), denoted 3, 4, and 5, with [Chl] = 1.75, 1.08, 5.45 mg m^{-3}, respectively. (c) Detail of the spectral zone 625–725 nm, which includes the fluorescence peak (logarithmic scale). The successive panels are for increasing depth as indicated; solid curves, upward irradiance; dashed curves (from z = 21.2 m and beyond), downward irradiance. At this station (150 °W–1 °S, 14 November 1994), [Chl] is steadily 0.25 (±0.02) mg m^{-3} within the entire water column.

and Lu683 as recorded at an OLIPAC station (see the figure caption) where the [Chl] was constant (0.18 mg m^{-3}) down to 55 m and then increased to a maximum of 0.29 mg m^{-3} at 60–75 m. As is clearly shown by these records, the Lu683 signal is drowned within the elastically backscattered sunlight in the upper layer down to ~12 m. Beyond this depth, when the background has vanished, the inelastic signal decreases slowly. The slope of this decrease (between 15 and 55 m) is distinctly less than that of the PAR decrease (K_{PAR} is ~0.048 m^{-1}). This difference presumably originates from attenuation of the blue and blue-green radiation absorbed by algae and exciting the fluorescence emission, which is less than the attenuation for the entire PAR domain. Note that an increase in the fluorescence quantum yield may also occur and could explain the slope divergence. The maximum in the L_u profile that occurs at 60 m coincides with the biomass maximum. Beyond 75 m, where K_{PAR} decreases progressively from 0.052 m^{-1} at the level of the DCM to 0.037 m^{-1} (at 100 m), Lu683 decreases in a steeper manner than does PAR, essentially as a result of the progressive diminution of algal biomass.

An example of downward and upward irradiance spectra measured at the same location and depth is shown in Fig. 2(a). The fluorescence emission is clearly detected in both records, with similar peak heights above different backgrounds. In Fig. 2(c) an enlargement of the spectra in the 625–725 nm domain is also provided; these irradiance measurements were carried out at various depths in another station selected because the [Chl] vertical profile was uniform. As anticipated [Eq. (10)], the fluorescence peak within the downward radiant flux is systematically above that which emerges from the upward flux. The peak height decreases along with the depth according to an attenuation coefficient of ~0.038 m^{-1} (30.8–61.2 m), approximately equal to the mean K coefficient for blue and green downward exciting radiation and thus slightly smaller than K_{PAR} (which amounts to 0.046 m^{-1}).

When the depth increases, the upward fluorescence signal becomes increasingly detached from the background. Below the 15-m depth, the upward irradiance measured on the short-wavelength side of the peak (within the 650–660-nm band) is due exclusively to inelastic Raman scattering. With increas-

ing depth, the decrease of this Raman signal is more accentuated than the decrease in the fluorescence peak itself. This is a consequence of an attenuation of the radiation that is able to excite the Raman emission (a band near 550 nm), which is stronger than the attenuation that affects the blue-green radiation (which is predominant in exciting the chlorophyll fluorescence). As a consequence, the fluorescence peak generally becomes more prominent above the background when depth increases.

The situation is similar for the peak detected in the downward flux, except that the transmitted sunlight also contributes to the downward irradiance within the 650–660-band and thus to the formation of the background (down to ~35 m in the instance shown). Beyond this depth, the transmitted radiation is vanishingly low, so the background also becomes a pure Raman scattering signal, as in the upward radiative field; note that the downward Raman signal generated by the upper layers is larger than the upward signal, for the same reason as was already explained for fluorescence.

Several examples of the fluorescence emission as detected in the upward flux, just beneath the surface, are shown in Fig. 2(b). OLIPAC and PACIPROD data, with [Chl] varying over a wide range (see the caption to Fig. 2) are displayed together, in terms of spectral reflectance $R(\lambda)$, defined as the ratio $E_u(\lambda)/E_d(\lambda)$. Such R(λ) spectra are independent of the level of incident irradiance and thus directly comparable in shape and magnitude. The prominent fluorescence peak associated with high biomasses (Peruvian upwelling) reduces to a small, albeit noticeable, peak in oligotrophic waters (tropical Pacific).

As proposed by Gordon[4] for reflectance spectra, or by Kishino *et al.*[6] for upward irradiance spectra, one can operationally quantify the fluorescence emission by considering the fluorescence peak after having adopted a baseline, assumed to represent the reflectance or the upward irradiance in the absence of fluorescence. The rather monotonic increase of water absorption within this spectral interval allows a straight line (in linear coordinates) to be adopted as a convenient baseline. In what follows, the straight line drawn from 655 to 710 nm is systematically used, and the same procedure is applied to upward as well as downward irradiance spectra. These wavelengths were adopted after a careful visual inspection of the records and also because they are symmetrical (±27.5 nm) about the peak (682.5 nm) and distant enough to capture the whole fluorescence emission.

The integral of the spectrum above this baseline represents the amount of energy emitted through fluorescence. The integral below this line represents the background. For the upwelling spectra, the background originates from Raman emission or, at shallow depth, from Raman plus elastically backscattered radiation. In the case of downwelling irradiance, the transmitted radiation, when it is still present, is also included in the background. Note that, for the deepest experiments, drawing a baseline may in practice become problematic, as the wings of the peak are swamped within the instrumental noise [see the deepest measurements in Fig. 2(c)]. Therefore all peaks, baselines, and corresponding integrals have to be visually controlled on a case-by-case basis before adoption or rejection. Rejection was inevitable when the peak was not well delineated or did not emerge sufficiently from the background, as generally occurred in oligotrophic waters when the [Chl] was below ~0.07 mg m^{-3}.

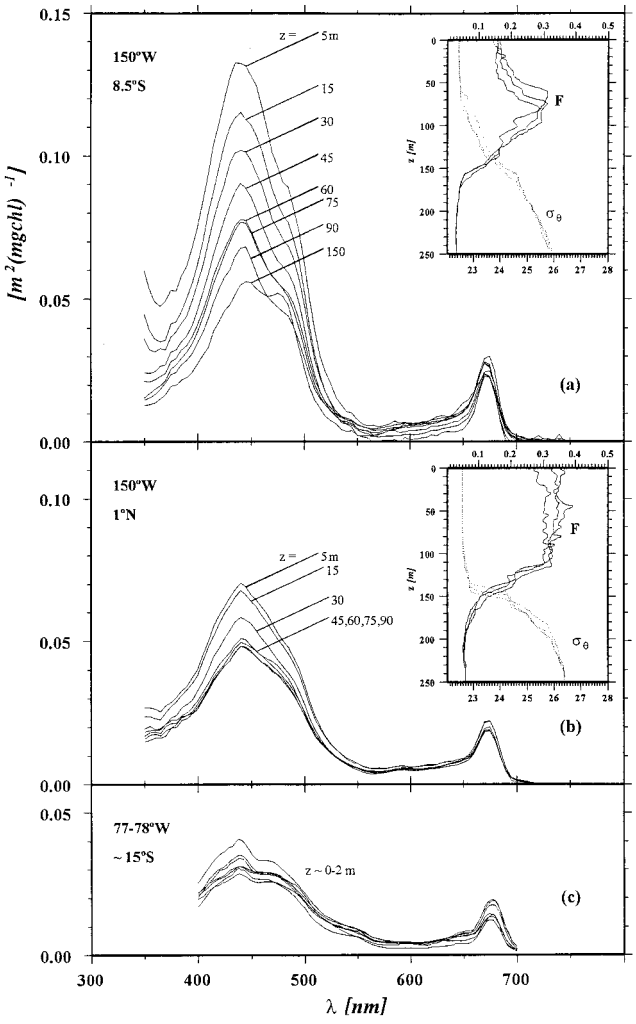

Fig. 3. Examples of chlorophyll-specific absorption spectra of algae in three situations (a) in oligotrophic waters, (b) in mesotrophic waters (OLIPAC cruise), (c) in eutrophic waters (PACIPROD cruise) in the Peruvian upwelling zone.[20] For (c), only near-surface waters samples are shown; for (a) and (b), the sampling depths are indicated, together with the SeaTech fluorescence and density profiles.

Extreme examples of chlorophyll-specific absorption spectra (Fig. 3) have been selected to illustrate the variability in magnitude of these coefficients, which directly affects the computation of the absorbed energy [Eq. (2)]. This variability for the OLIPAC samples has already been discussed in detail elsewhere.[31] Suffice it to recall that, in oligotrophic stratified waters, the presence of nonphoto-

synthetic pigments (such as zeaxanthin) induces a drastic enhancement of $a^*(\lambda)$ in the blue part of the spectrum [Fig. 3(a)], particularly for the upper layer samples, and then a regular decrease of specific absorption with increasing depth. In contrast [Fig. 3(b)], in mesotrophic and in well-mixed waters, the $a^*(\lambda)$ values are considerably lower and do not vary widely with depth. In the eutrophic waters of the Peruvian upwelling [Fig. 3(c)], low $a^*(\lambda)$ values, which are typical of large algal cells,[17,32] are systematically found at all depths (only surface samples are shown).

5. Results

A. Estimates of the Quantum Yield from the Spectroradiometer Data

We isolated the fluorescence signals $E_{f\uparrow}$ and $E_{f\downarrow}$ considered below from the upward and downward irradiance spectra by subtracting the background, as explained above. Even if only $E_{f\uparrow}(z)$ is considered for the computation of ϕ [Eq. (7)], $E_d(\lambda, z)$ must still be known and convoluted with the algal absorption spectrum [Eq. (2)] to yield the amount of absorbed energy. Therefore ϕ cannot be derived for the upper layers, to the extent that it was not possible to determine $E_d(\lambda, z)$. For the layer closest to the surface, however, a possibility of extracting ϕ from the upward irradiance measured just beneath the surface does exist and is examined below. The results for the OLIPAC cruise, obtained through Eq. (7) and based on $E_{f\uparrow}$ only, are given in chronological–geographical order in Fig. 4(a). Distinct symbols approximately indicate the corresponding depths (including the near surface). In Fig. 4(b) the same ϕ values are plotted as a function of depth for each station; the latitudes are given for those profiles that exhibit particularly high or low values. The fluorescence yield at the same depths can also be derived from the downward field [Eq. (8)]. The quantum yield estimates derived from the upward fluorescence signals are in excellent agreement (Fig. 5) with those derived from the (independent) downward measurements, which reinforce the confidence in the results. This agreement is also reflected by the fact that Eq. (9) is rather well verified, at least within the accuracy expected from measurements of such weak signals and when one considers the unavoidable uncertainties that result from the delineation and extraction of the background. Indeed, the mean value (all depths pooled together) of the ratio $E_{f\downarrow}(z)/E_{f\uparrow}(z)$ is 1.13 ($\pm$0.12 at one standard deviation and $N = 55$), whereas the predicted value [Eq. (9)] is 1.11 (=0.80/0.72), according to the mean coefficients adopted.

B. Estimates of the Quantum Yield from the Profiler Data

The computation of the quantum yield of fluorescence based on the PNF 300 data makes use of Eq. (6). Nevertheless, this derivation is not straightforward to the extent that $\bar{a}_{ex}$ is not known. Beside knowledge of the algal absorption spectrum, the computation of a^*_{ex} also requires knowledge of the spectral

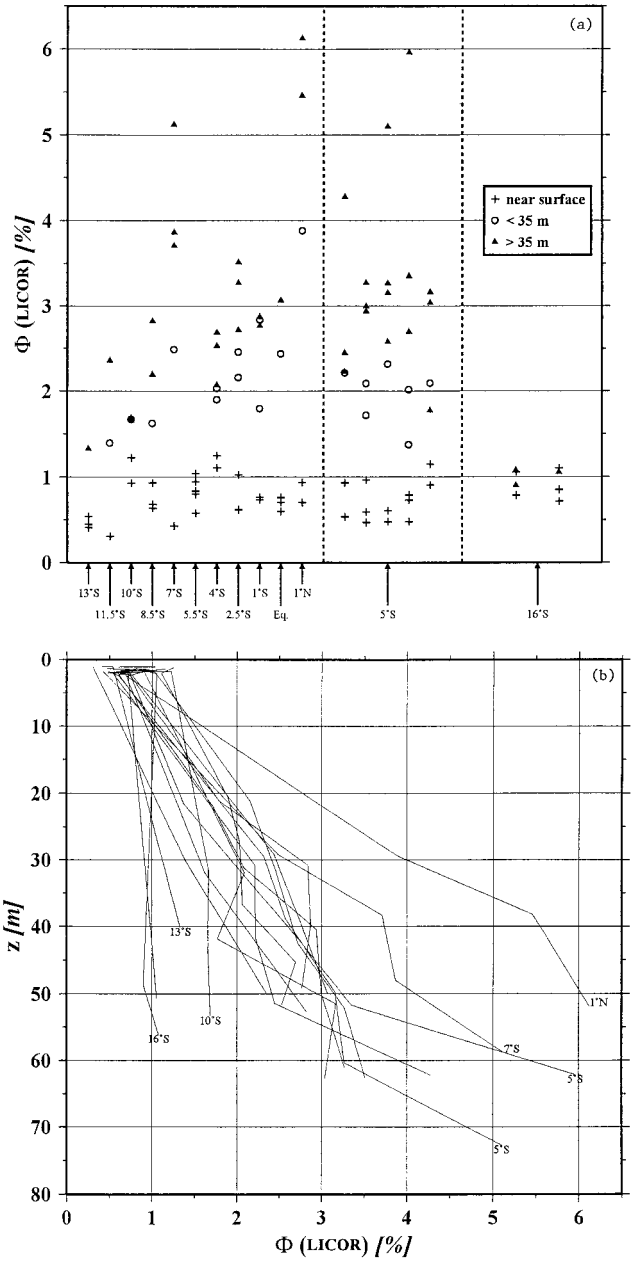

Fig. 4. (a) Fluorescence quantum yields ϕ derived from the LI-1800 UW (LiCor) upwelling irradiance data at all stations all along 150 °W and at latitudes as indicated (the increment in the x axis actually corresponds to 1 day; 5-day stations were occupied at 5° and 16 °S). Symbols represent the depth of the ϕ estimates. (b) Same data as in (a) displayed for each station as a function of depth. Stations with particularly high or low ϕ are indicated by their latitude (longitude is always 150 °W).

distribution of the light that is available at the depth considered. Practically, a^*_{ex} is computed with Eq. (2″), where the spectral $E(\lambda)$ values (not measured) are replaced by $E_d(\lambda)$ measured at the same depth with the LI-1800 UW instrument. Finally, one obtains the absorbed radiation by using $E_{ex}(z)$ (actually PAR) measured with the PNF 300 sensor and then reassembling these quantities according to Eq. (2′). Using the quantity $[E_d(\lambda) + E_u(\lambda)]$ rather than solely

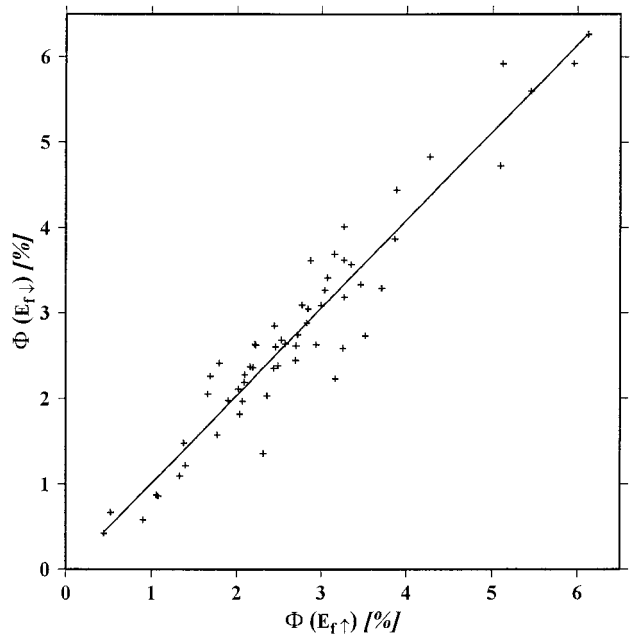

Fig. 5. Quantum yield (Y) derived from the downward fluorescence signals [Eq. (7)] as a function of yield (X) from the upward signal [Eq. (6)] at the same depths and stations. Linear regression, $Y = 1.027X - 0.02$ (with $r^2 = 0.913$). The regression (plot not shown) between the quantum yield derived from the sum of the upward and downward fluorescence signals [through Eq. (9)] and that derived from the downward signal practically leads to a 1:1 line, with a higher r^2 (=0.973).

$E_d(\lambda)$ when computing a^*_{ex} would be in principle more accurate, but this refinement has no practical effect (less than 1%) on the resultant a^*_{ex} value. Resorting to $E_d(\lambda)$ as a substitute for $\hat{E}(\lambda)$ limits the exploitation of the PNF data to those depths where the LI-1800 UW spectral data were obtained. The comparison below is made on the basis of these discrete measurements only. A possible interpolation procedure by which the above limitation can be practically removed under some assumptions is presented in Subsection 5.E.

C. Comparison of the Two Estimates

In the clear Pacific waters investigated, the two series of ϕ estimates (from the LI-1800 UW and the PNF 300 data) can be compared within the 20–63-m depth range for the following reasons: As was already said, the backscattered radiation contaminates the Lu683 signal down to ~15 m; anyway, $E_d(\lambda)$ cannot be measured at depths less than 20 m. Because of the sensitivity limitation of the LI-1800 UW instrument, the fluorescence peak cannot be quantitatively extracted from the noise that affects the downward or upward irradiance spectra when the depth exceeds 65 m in the clearest waters, so a comparison with the PNF 300-based estimates is no longer possible.

At 20 m or deeper, the inevitable inclusion of the (Raman) background in the Lu683 signal results in an overestimate of the fluorescence quantum yield if this signal is exploited without caution. In fact, it is possible to evaluate the contribution of the Raman scattering to the total signal recorded in the red band by taking advantage of the contemporaneous spectral irradiance measurements. As explained above, it suffices to compare the integrals when one is excluding or including the background. As a result of such comparisons, it follows that the Raman background amounts to values that generally comprise 25–35% of the total signal recorded by the LI-1800 UW instrument within the 655–710-nm band. These numbers can be used, case by case, for correcting the PNF 300 data from the unwanted contribution (which varies with depth) and thus for deriving Raman-corrected fluorescence yields. Whereas the PNF 300 instrument can easily detect a significant Lu683 signal at great depth (actually detected down to 160 m), removal of the Raman background, which rests on the use of the spectroradiometer, cannot be achieved for such depths.

We acknowledge that, at great depth, the relative contribution of the Raman emission is considerably reduced. Indeed, this contribution (given a uniform chlorophyll profile, for example) decreases for increasing depth because the attenuation of the blue radiation exciting the fluorescence is smaller than that of the green radiation (near 550 nm), which excites the Raman scattering near 683 nm. As a consequence, a significant Lu683 signal recorded at great depth can safely be attributed to the sole chlorophyll fluorescence (for example, within the DCM layer found at 120–160 m in oligotrophic waters at 16 °S, 150 °W). At intermediate depths, when the Raman emission has not yet vanished its relative contribution obviously depends on the chlorophyll concentration, which determines the magnitude of the fluorescence emission. As a consequence, the unwanted contribution increases for decreasing [Chl] in oligotrophic environments. When the Raman contribution exceeded 35%, inaccurate (and therefore discarded) ϕ values at intermediate depths were computed when the [Chl] was below 0.07 mg m^{-3}. Note that, for this specific reason, only a few data for the oligotrophic station at 16 °S are shown in Fig. 4(a).

The ϕ values derived for the same depths by use of the Lu683 signal, or by use of the $E_{f\uparrow}$ signal estimated from the LI-1800 UW data, are comparatively displayed in Fig. 6. We show the ϕ(PNF) values, before the Raman contribution is removed, to illustrate the importance of this correction. As the depth does not exceed 63 m in this comparison, the Raman contribution actually was never negligible for these instances. After the correction is effected, both estimates are brought back very close together, with a 1-to-1 relationship (when the five highest values are discarded).

D. Quantum Yield in the Near-Surface Layer

The Lu683 sensor is inoperative inside the near-surface layer, as it captures essentially backscattered radiation. The quantum yield for fluorescence can nevertheless be computed [Eq. (7)] from the spectral upward irradiance measured with the LI-1800 UW

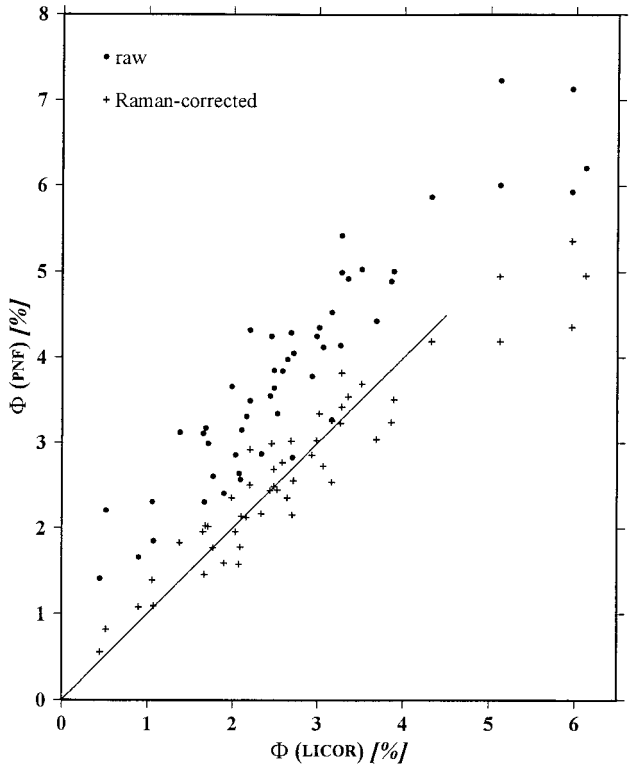

Fig. 6. Quantum yield values derived from the PNF 300 instrument (PNF), without (raw) or after Raman correction as a function of those derived from the upward fluorescence signal determined with the LI-1800 UW (LI-COR) instrument; when the five ϕ(LI-COR) values that exceed 5% are excluded, the slope of the regression line (solid line) is 0.995, and $r^2 = 0.98$.

instrument just below the surface (generally at a variable depth near 1 m). Within this irradiance spectrum, the $E_{f\uparrow}$ signal can be isolated and quantified above the baseline; then it can be associated with the downward irradiance spectrum recorded above the surface after due correction. The correction includes two terms, namely, the loss by reflection at the interface (a constant transmission factor equal to 0.95 is adopted) and the geometric factor that accounts for the redistribution of radiant energy, i.e., the transformation of downward plane irradiance into a scalar irradiance. For the latter effect, a mean value of 1.20 is adopted. The rapid change in the spectral distribution of exciting radiation within the successive upper thin layers that contributes to the fluorescence emission is another complication, which is simply ignored [that means that K in Eq. (4) or Eq. (5) is not made dependent on the distance x]. Therefore the yield values are admittedly approximate.

This method is used for the OLIPAC data with low or moderate [Chl] and also for the PACIPROD data, which exhibit huge fluorescence peaks owing to the presence of much higher algal biomasses [Fig. 2(b)]. The near-surface fluorescence quantum yields in the OLIPAC stations are dramatically less (by factors of 3–5) than the yields determined at depth, and this depression quantifies the importance of photoinhibition processes. The near-surface ϕ values for this cruise, as displayed in Fig. 4, lead to an average value of 0.84% ($\pm$0.26 at one standard deviation, with N = 43). It is worth noting that all these values correspond to measurements made near solar noon, with incident PAR values from 350 to 450 W m^{-2} above surface (or 1600 and 2000 μmol. quanta m^{-2} s^{-1}, approximately). The results for the PACIPROD cruise (not displayed) lead to an average value above those of OLIPAC, namely, 1.53% ($\pm$0.4, with N = 11). It is worth noting that, during this cruise, the incident PAR values were generally half of those cited above. In three specific instances, when measurements were made under heavily overcast conditions ($\sim$200 μmol quanta m^{-2} s^{-1}), even higher values, namely, 2.9%, 3.1%, and 4.3%, were derived.

E. Full Profiles of the Quantum Yield from the Profiler Data

As was already strongly suggested by the profiles in Fig. 4(b), the fluorescence quantum yield distinctly increased with increasing depth for all stations of the OLIPAC cruise. This preliminary observation, based on discrete estimates, can be more thoroughly documented by use of the PNF 300 continuous profiles, even if the approach is necessarily less rigorous. Indeed, some interpolations, and associated assumptions of continuity within the water column, are needed if one is to make use of all the information contained in the vertical Lu683 profiles.

The approach consists of operating Eq. (2″) and computing $\bar{a}^*_{ex}$ each time that it is possible. In fact, at each depth at which a chlorophyll-specific absorption spectrum has been measured (nominally at eight depths from 5 to 105 m) and [Chl] determined, the appropriate E_d spectrum is known or obtained by interpolation); then A_{ex}, the amount of absorbed energy, can be computed. By interpolating among these eight levels one can continuously express A_{ex} as a function of depth, and thus it becomes possible to transform the fluorescence profile (binned every 5 m) into a quantum yield profile. Again, the ϕ values must be corrected for the Raman emission. Examples of full profiles of ϕ are provided in Fig. 7, where three typical situations are presented. The first one is characterized by a vertically homogeneous biomass (down to 90 m; Fig. 7, inset). In the second situation the vertical profile exhibits a broad DCM, and for the third station, in stratified oligotrophic waters, the DCM occurs much deeper (145 m).[21]

Despite the absence of stratification and vertical structures in the first situation, the ϕ profile is strongly and regularly featured, with maximal values near 70 m. This suggests that the shape of this profile would essentially result from physiological adjustments to the radiative level and that these adjustments are made quickly (at least compared with the time scale of the possible vertical motions inside such a well-mixed layer). In the second situation, the ϕ profile is similar, apart from its asymmetrical shape, which is likely associated with the vertically

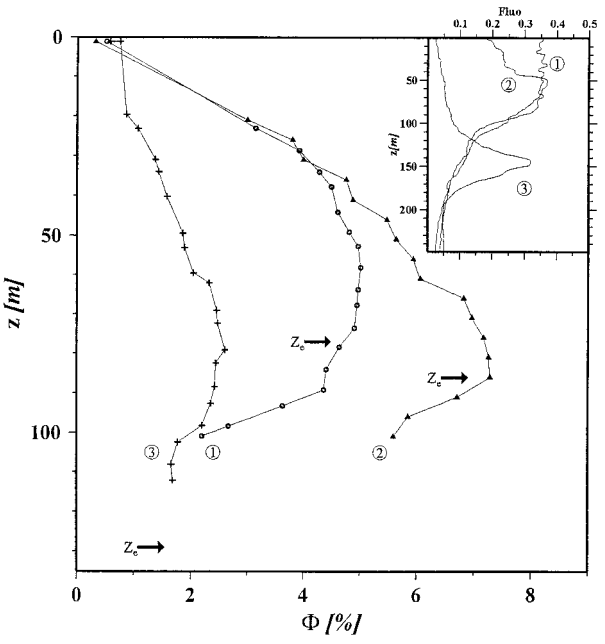

Fig. 7. Raman-corrected quantum yield derived from the PNF 300 profiles (see text). The three examples, along the 150 °W meridian, are (1) for a station at the equator on 15 November 1984, (2) for a station at 5 °S on 21 November 1984, and (3) at 16 °S on 26 November 1984. The SeaTech fluorescence profiles, determined at these stations early in the morning (before photoinhibition starts), are shown in the inset to illustrate roughly the vertical biomass distribution; the [Chl] values are constant from 0 to 90 m and are equal to 0.29 mg m^{-3} for example (1); for example (2) they are 0.17 and 0.28 mg m^{-3} within the upper layers and inside the DCM, respectively; for the third example, they are 0.035 and 0.29 mg m^{-3} near the surface and inside the DCM.

structured algal distribution. The maximum in ϕ, which occurs at 85 m, is below the DCM (lying from 50 to 80 m). The converse is true for the third situation, as the ϕ smooth maximum (at 80 m) is well above the DCM. In this ultraoligotrophic situation, the entire profile is characterized by distinctly lower ϕ values, even if its convex shape is rather similar to that found in the second situation. If (hypothetically) the general shape of the profile is to be related to irradiance levels, it must be noted that the position of the ϕ maximum does not coincide with a well-defined optical depth. Indeed, at the level where ϕ experiences its maximum, the PAR is reduced to approximately 3%, 1%, and 6% of its surface value at the three stations, respectively. If it exists, the link between availability of light and the level at which ϕ experiences its maximum is not tight. However, at least for the first two stations in Fig. 7, ϕ decreases abruptly below the euphotic depth, Z_e (the 1% PAR level).

6. Discussion and Conclusions

It is somewhat useless to compare the present estimates of the quantum yield with already published values inasmuch as, in previous studies, the magnitude and the spectral dependence of the *in vivo* absorption coefficient for algae were assumed, whereas in the present study the crucial quantity expressed by Eq. (2) was assessed in a rather accurate way and on a case-by-case basis. Nonetheless, it is worth noting that the low ϕ values derived by Gordon[4] or by Kattawar and Vastano[5] from spectral reflectance just beneath the surface and by use of a mean algal absorption spectrum are approximately similar to those found here within the upper layer. As the determinations were made near local noon under maximal incoming radiation, the ϕ values are depressed. The ϕ diel variations are in opposite phase with respect to the solar irradiance cycle,[16] and the depression near noon results mainly from nonphotochemical quenching.[33,34] This effect is obviously maximal for the near-surface ϕ values. At depth, ϕ increases with values regularly distributed along the vertical (Fig. 7). The present deep values, generally 2–3% and reaching 5–6% in a few instances, are considerably lower than those reported by Kishino *et al.*,[7] who found values of 6–12% in open ocean and for the layer located below the 10% PAR level.

In oligotrophic waters [13° and 16 °S in Fig. 4(a) or profile 3, in Fig. 7], the fluorescence yield is always low and increases by only a factor of 2 from surface to depth. The algal population in these waters, dominated by *Prochlorococcus*,[21] exhibits high chlorophyll-specific absorption [Fig. 3(a)], mainly in response to the presence of abundant nonphotosynthetic pigments (such as zeaxanthin and diadinoxanthin[31]). Such pigments do not transfer to chlorophyll molecules the energy that they have absorbed; therefore more energy is dissipated as heat, and the fluorescence quantum yield is accordingly reduced. In contrast, in eutrophic waters dominated by diatoms, with low chlorophyll-specific absorption [Fig. 3(c)] and no photoprotectant pigments, the energy transfer is efficiently performed by accessory pigments, and the fluorescence yield is higher, even in the near-surface layer (PACIPROD data). From south to north [Fig. 4(a)], and for waters becoming progressively mesotrophic (at 5–7 °S and again near the equator), intermediate absorption capacities occur; they are typical of the mixed populations (mainly picoeucaryotes and variable and lesser proportions of *Prochlorococcus* and *Synechococcus*) encountered in these mesotrophic situations.[21] The yield at the surface remains low, but it increases by a factor of 5, or even of 10, at depth [Fig. 4(a); Fig. 7, profiles ① and ②]. Such an increase, no longer related to the pigment composition and change in absorption capacities [they are rather stable; see Fig. 3(b)], is more likely to be associated with a change in photochemistry and perhaps in the sharing of chlorophyll molecules between photosystems I and II (recall that fluorescence emission originates only from photosystem II).

More-elaborate interpretations of the ϕ values in terms of photophysiology are beyond the scope of the present study (but see Kiefer and Reynolds[35]) and will be possible after systematic determinations have

been made for various phytoplanktonic assemblages in diversified physical or chemical forcing conditions. It is worth noting that studying this yield requires the full suite of *in situ* (spectral irradiance) and *in vitro* (spectral absorption) measurements, which, not surprisingly, are the same as those required for a meaningful interpretation of the quantum yield for photosynthesis. The very purposes of the present methodological study were to demonstrate that the chlorophyll fluorescence signal can be measured accurately in the upward and downward radiant fields and that the value of the *in situ* quantum yield can be derived without interference from the Raman emission (provided that the full spectral information has been simultaneously acquired). This study has also shown that the variations of quantum yield with depth and location are well organized. Systematic field studies can thus be performed, and, on this basis, physiological interpretation and ecological application will be possible in the future.

In the perspective of remote-sensing applications, only the fluorescence yield in the upper layer is needed, as the emerging signal that is detectable from space originates from a rather thin layer (see, e.g., Babin *et al.*[16]). This yield remains low, near 1%, according to the present measurements, which admittedly were performed when the solar irradiance was close to its maximum and when the diel variation of fluorescence yield passed through its minimum. Note that the equator crossing time for most of the ocean color sensors is never far from midday, so the ϕ value involved in remote sensing corresponds to clear-sky conditions near noon. Predicting or interpreting the fluorescence signal as possibly captured from space still requires assumptions or additional measurements for documenting the variability of the near-surface ϕ value.

Instead of expensive hyperspectral instruments, a simple arrangement with three channels could be an adequate solution for field measurements at sea. With two channels to establish the baseline and a central channel to measure the fluorescence signal above the baseline, it would still be possible to correct for the Raman emission and backscattered radiation. One can use incident spectral irradiance, measured above the surface or modeled, to infer the exciting radiation within the upper layer, without significant error. Finally, it should be emphasized that, when one is studying the photophysiology of natural populations, as well as for remote-sensing applications, the information needed is the *in situ* fluorescence quantum yield as realized under natural illumination conditions. However, most of the information currently available originates from experiments that involve various artificial light sources and often a transfer of samples. When the fast response of the photosynthetic apparatus is considered, such information may be notably insufficient when one is trying to interpret *in situ* processes and phytoplanktonic assemblages. For this reason, and with this purpose, a nonintrusive method is indubitably more relevant.

We thank A. Bricaud and K. Allali for providing the PACIPROD and OLIPAC absorption data and D. Tailliez for the density and SeaTech fluorescence data. We are grateful to M. Babin, D. A. Siegel, and an anonymous referee for their helpful comments.

References

1. J. E. Tyler and R. C. Smith, *Measurements of Spectral Irradiance under Water*, Vol. 1 of Ocean Series (Gordon & Breach, New York, 1970), p. 103.
2. R. A. Neville and J. F. R. Gower, "Passive remote-sensing of phytoplankton via chlorophyll-alpha fluorescence," J. Geophys. Res. **82,** 3487–3493 (1977).
3. A. Morel and L. Prieur, "Analysis of variations in ocean color," Limnol. Oceanogr. **22,** 709–722 (1977).
4. H. R. Gordon, "Diffuse reflectance of the ocean: the theory of its augmentation by chlorophyll *a* fluorescence at 685 nm," Appl. Opt. **18,** 1161–1166 (1979).
5. G. W. Kattawar and J. C. Vastano, "Exact 1-D solution to the problem of chlorophyll fluorescence from the ocean," Appl. Opt. **21,** 2489–2492 (1982).
6. M. Kishino, S. Sugihara, and N. Okami, "Influence of fluorescence of chlorophyll *a* on underwater upward irradiance spectrum," La Mer **22,** 224–232 (1984).
7. M. Kishino, S. Sugihara, and N. Okami, "Estimation of quantum yield of chlorophyll *a* fluorescence from the upward irradiance spectrum in the sea," La Mer **22,** 233–240 (1984).
8. D. A. Kiefer, W. S. Chamberlin, and C. R. Booth, "Natural fluorescence of chlorophyll *a*: relationship to photosynthesis and chlorophyll concentration in the western South Pacific gyre," Limnol. Oceanogr. **34,** 868–881 (1989).
9. P. G. Falkowski and D. A. Kiefer, "Chlorophyll *a* fluorescence in phytoplankton: relationship to photosynthesis and biomass," J. Plankton Res. **7,** 715–731 (1985).
10. W. S. Chamberlin, C. R. Booth, D. A. Kiefer, J. H. Morrow, and R. C. Murphy, "Evidence for a simple relationship between natural fluorescence, photosynthesis and chlorophyll in the sea," Deep-Sea Res. **37,** 951–973 (1990).
11. B. J. Topliss and T. Platt, "Passive fluorescence and photosynthesis in the ocean—implications for remote-sensing," Deep-Sea Res. **33,** 849–864 (1986).
12. T. G. Owens, "Energy transformation and fluorescence in photosynthesis," in *Particle Analysis in Oceanography*, S. Demers, ed. (Springer-Verlag, Berlin, 1991), pp. 101–137.
13. G. H. Krause and E. Weis, "Chlorophyll fluorescence and photosynthesis—the basics," Annu. Rev. Plant Phys. **42,** 313–349 (1991).
14. J. F. R. Gower and G. A. Borstad, "Use of *in vivo* fluorescence line at 685 nm for remote sensing surveys of surface chlorophyll *a*," in *Oceanography from Space*, J. F. R. Gower, ed. (Plenum, New York, 1981), pp. 329–338.
15. M. R. Abbott and R. M. Letelier, "Chlorophyll fluorescence (MODIS Product Number 20)," MODIS algorithm theoretical basis document (http://modis.gsfc.nasa.gov/MODIS/ATBD, 1999).
16. M. Babin, A. Morel, and B. Gentili, "Remote sensing of sea surface Sun-induced chlorophyll fluorescence: consequences of natural variations in the optical characteristics of phytoplankton and the quantum yield of chlorophyll *a* fluorescence," Int. J. Remote Sens. **17,** 2417–2448 (1996).
17. A. Bricaud, M. Babin, A. Morel, and H. Claustre, "Variability in the chlorophyll-specific absorption coefficients of natural phytoplankton: analysis and parameterization," J. Geophys. Res. **100,** 13,321–13,332 (1995).
18. A. Bricaud, A. Morel, M. Babin, K. Allali, and H. Claustre, "Variations of light absorption by suspended particles with chlorophyll *a* concentration in oceanic (case 1) waters: anal-

ysis and implications for bio-optical models," J. Geophys. Res. **103,** 31,033–31,044 (1998).
19. M. Kishino, M. Takahashi, N. Okami, and S. Ichimura, "Estimation of the spectral absorption coefficients of phytoplankton in the sea," Bull. Mar. Sci. **37,** 634–642 (1985).
20. A. Bricaud and D. Stramski, "Spectral absorption-coefficients of living phytoplankton and nonalgal biogenous matter—a comparison between the Peru upwelling area and the Sargasso Sea," Limnol. Oceanogr. **35,** 562–582 (1990).
21. H. Claustre, A. Morel, M. Babin, C. Cailliau, D. Marie, J.-C. Marty, D. Tailliez, and D. Vaulot, "Variability in particle attenuation and chlorophyll fluorescence in the tropical Pacific: Scales, patterns, and biogeochemical implications," J. Geophys. Res. **104,** 3401–3422 (1999).
22. Y. Dandonneau, "Introduction to special section: biogeochemical conditions in the equatorial Pacific in late 1994," J. Geophys. Res. **104,** 3291–3295 (1999).
23. B. Coste, H. J. Minas, and M. C. Bonin, "Production Pélagique des Côtes du Pérou et des Iles Galapagos, Campagne PACIPROD (8 Aout–18 Septembre 1986)," Campagnes Oceanographiques Francaises, Rap. 7 (Institut Français de Recherche pour l'Exploitation de la Mer, Service Documentation and Publications, Plouzane, France, 1987), p. 183.
24. A. Morel, "Optical modeling of the upper ocean in relation to its biogenous matter content (Case I waters)," J. Geophys. Res. **93,** 10,749–10,768 (1988).
25. D. J. Collins, D. A. Kiefer, J. B. SooHoo, and I. S. McDermid, "The role of reabsorption in the spectral distribution of phytoplankton fluorescence emission," Deep-Sea Res. **32,** 983–1003 (1985).
26. R. M. Pope and E. S. Fry, "Absorption spectrum (380–700 nm) of pure water. II. Integrating cavity measurements," Appl. Opt. **36,** 8710–8723 (1997).
27. J. T. O. Kirk, "The upwelling light stream in natural waters," Limnol. Oceanogr. **34,** 1410–1425 (1989).
28. S. Maritorena, A. Morel, and B. Gentili, "Diffuse reflectance of oceanic shallow waters: influence of water depth and bottom albedo," Limnol. Oceanogr. **39,** 1689–1703 (1994).
29. B. R. Marshall and R. C. Smith, "Raman scattering and in-water ocean optical properties," Appl. Opt. **29,** 71–84 (1990).
30. A. Morel and H. Loisel, "Apparent optical properties of oceanic water: dependence on the molecular scattering contribution," Appl. Opt. **37,** 4765–4776 (1998).
31. K. Allali, A. Bricaud, and H. Claustre, "Spatial variations in the chlorophyll-specific absorption coefficients of phytoplankton and photosynthetically active pigments in the equatorial Pacific," J. Geophys. Res. **102,** 12,413–12,423 (1997).
32. C. S. Yentsch and D. A. Phinney, "A bridge between ocean optics and microbial ecology," Limnol Oceanogr. **34,** 1694–1705 (1989).
33. J. Marra, "Analysis of diel variability in chlorophyll fluorescence," J. Mar. Res. **55,** 767–784 (1997).
34. P. G. Falkowski and J. A. Raven, *Aquatic photosynthesis* (Blackwell, Malden, Mass., 1997), p. 375.
35. D. A. Kiefer and R. A. Reynolds, "Advances in understanding phytoplankton fluorescence and photosynthesis," in *Primary Productivity and Biogeochemical Cycles in the Sea*, P. G. Falkowski and A. D. Woodhead, eds. (Plenum, New York, 1992), pp. 155–179.